Processing of progranulin into granulins involves multiple lysosomal proteases and is affected in frontotemporal lobar degeneration

Swetha Mohan
University of California San Francisco
Paul J. Sampognaro
University of California San Francisco
Andrea R. Argouarch
University of California San Francisco
Jason C. Maynard
University of California San Francisco
Anand Patwardhan
University of California San Francisco
Emma C. Courtney
University of California San Francisco
Amanda Mason
University of California San Francisco
Kathy H. Li
University of California San Francisco
William W. Seeley
University of California San Francisco
Bruce L. Miller
University of California San Francisco
Alma Burlingame
University of California San Francisco
Mathew P. Jacobson
University of California San Francisco
Aimee Kao (Aimee.Kao@UCSF.EDU)
University of California San Francisco https://orcid.org/0000-0002-7686-7968

Research article

Keywords: Progranulin, granulin, frontotemporal lobar degeneration, lysosome, protease, pH, asparagine endopeptidase

Posted Date: July 22nd, 2020

DOI: https://doi.org/10.21203/rs.3.rs-44128/v1

Version of Record: A version of this preprint was published at Molecular Neurodegeneration on August 3rd, 2021. See the published version at https://doi.org/10.1186/s13024-021-00472-1.

Abstract

Background: Progranulin loss-of-function mutations are linked to frontotemporal lobar degeneration with TDP-43 positive inclusions (FTLD-TDP-*Pgrn*). Progranulin (PGRN) is an intracellular and secreted pro-protein that is proteolytically cleaved into individual granulin peptides, which are increasingly thought to contribute to FTLD-TDP-*Pgrn* disease pathophysiology. Intracellular PGRN is processed into granulins in the endo-lysosomal compartments. Therefore, to better understand the conversion of intracellular PGRN into granulins, we systematically tested the ability of different classes of endo-lysosomal proteases at a range of pH setpoints.

Results: *In vitro* cleavage assays identified multiple enzymes that can process human PGRN into multi- and single-granulin fragments in a pH-dependent manner. We confirmed the role of cathepsin B and cathepsin L in PGRN processing and showed that these and several previously unidentified lysosomal proteases (cathepsins E, G, K, S and V) are able to process PGRN in variable, pH-dependent manners. In addition, we have demonstrated a new role for asparagine endopeptidase (AEP) in processing PGRN, with AEP having the unique ability to liberate granulin F from the pro-protein. Brain tissue from individuals with FTLD-TDP-*Pgrn* show increased PGRN processing to granulin F, correlating with increased activity of AEP, in a region-specific manner.

Conclusions: This study demonstrates that multiple lysosomal proteases may work in concert to liberate granulins and implicates both AEP and granulin F in the neurobiology of FTLD-TDP-*Pgrn*. Modulating progranulin cleavage may represent a new strategy to modulate PGRN and granulin levels in disease.

Background

Progranulin (PGRN) is an evolutionarily conserved glycoprotein with functions in inflammation, wound healing, tumorigenesis, and neuroprotection [1,2]. Dosage of PGRN plays a central role in its cellular functions as haploinsufficiency of PGRN leads to an adult-onset neurodegenerative disorder called frontotemporal lobar degeneration (FTLD-TDP-*Pgrn*) while complete loss of PGRN leads to a childhood lysosomal storage disorder called neuronal ceroid lipofuscinosis (NCL) [3-5]. As a molecule with complex layers of regulation, PGRN can also be proteolytically cleaved into multiple biologically active, disulfide-rich peptides known as granulins which, in some instances, have contrasting functions to its precursor [6-10]. Although granulins were identified before PGRN, the regulation of granulin production remains poorly understood [11]. Since haploinsufficiency of PGRN protein could potentially also affect granulin levels, understanding granulin production may shed light on how partial loss of PGRN causes age-associated neurodegeneration.

Proteolytic processing of PGRN liberates up to eight granulin peptides, named paragranulin (~3.5kD) and granulins A through G (~7kD each) (Fig. 1a). Fragments consisting of multiple granulins have also been previously described [12,13], and these multi-granulin fragments (MGFs) exert biological activities as well [14]. PGRN is secreted into the extracellular matrix where proteases, such as neutrophil elastase, may

process PGRN [6,8,15]. Intracellular PGRN localizes to the endo-lysosomes in multiple cell-types, and recent studies have shown that intracellular processing of PGRN into granulins also occurs in the endo-lysosomal compartments [16-20]. Consequently, lysosomal cysteine proteases, cathepsins B (CTSB) and L (CTSL), were identified as PGRN proteases in human and mouse models [17,19-20]. However, a comprehensive study of intracellular PGRN proteases has not yet been performed.

To better understand the intracellular processing of PGRN into granulins, we set out to catalog the endo-lysosomal proteases that can regulate PGRN processing into granulins. Using an *in vitro* protease cleavage assay, we identified multiple lysosomal proteases that can process PGRN to multi-granulin fragments and individual granulins. Interestingly, they did so in a pH-dependent manner that is distinctive for each protease. In a neuronal cell model, we validated the known roles for CTSB and CTSL and showed that asparagine endopeptidase (AEP, also known as legumain) is a novel PGRN protease that can specifically liberate granulin F. Finally, comparing human brain lysates from control and FTLD subjects, we show a significant increase in the production of granulin F in degenerating regions of the brain, correlating with increased activity of AEP. This study is the first to systematically identify a suite of endo-lysosomal proteases that may work in concert to process PGRN to granulins and reveals AEP as a new PGRN protease with relevance in FTLD-TDP. Better understanding of how PGRN haploinsufficiency affects PGRN processing may lead to new strategies for therapy.

Methods

In vitro cleavage assay

For *in vitro* cleavage assays, 400ng of recombinant human progranulin (R&D #CF-2420) was incubated with or without 1μM of each protease. Depending on the pH setpoint, the following buffers were used: 100mM sodium citrate pH 3.4, 50mM sodium acetate pH 4.5 or 5.5, 50mM 2-(N-morpholino)-ethanesulfonic acid (MES) buffer pH 6.5, 100mM phosphate buffer saline (PBS) pH 7.4 with 1mM EDTA and 2mM DTT for 20 or 60 minutes at 37ºC water bath. The cleavage was performed in a total volume to 19.5μl. Protease activity was stopped by adding 7.5μl of NuPAGE 4X LDS (Fisher #NP0007), 3μl of 10X reducing agent (i.e. 50μM) (Fisher #NP0009) and denatured for 10 minutes at 70ºC. Of note, we used these denaturing conditions to reduce the potential for dimerization of fragments (a known possibility with PGRN) [21]. The samples were run on precast NOVEX 4-12% Bis-Tris gels (Fisher #NP0321PK2) using MES buffer (Fisher #NP0002). The gel was then either fixed in 40% ethanol and 10% acetic acid for silver and coomaisse staining or transferred onto nitrocellulose membranes for western blotting analysis.

Silver stain - Silver staining was performed according to manufacturer's instructions with SilverQuest silver staining kit (Thermo #LC6070).

Coomassie stain - Coomassie staining was done using BIO-RAD QC colloidal coomaisse stain (Bio-rad #160-0803). The gel was stained overnight and was removed by washing in milli-Q water for 3 hours.

Recombinant proteases - Cathepsin E (R&D #1294-AS), Cathepsin D (R&D #1014-AS), Napsin A (R&D #8489-NA), Cathepsin G (Millipore #219873), Cathepsin A (R&D #1049-SE), Pro-X-carboxypeptidase (R&D #7164-SE-010), Cathepsin L (Millipore #219402), Cathepsin B (Millipore #219364), Cathepsin K (Millipore #219461), Cathepsin S (R&D #1183-CY), Cathepsin V (R&D #1080-CY), Asparagine endopeptidase/legumain (R&D #2199-CY), Cathepsin H (R&D #7516-CY-010), Cathepsin C (R&D #1071-CY), Cathepsin O (Abcam #ab267932), Cathepsin F (Abcam #ab240858), and Cathepsin X (R&D #934-CY).

Protease activation and confirmation of activity – Cathepsins E, D, G, L, B, K, S, V, F, and O as well as Asparagine endopeptidase, Napsin A, and Pro-X-carboxypeptidase require no activation, according to the vendor, and were used as purchased. Cathepsin A, C, and H require pre-activation before use. For cathepsin A and cathepsin C activation, 1μM of each protease was incubated with 200nM of cathepsin L at room temperature for 1 hour. After 1 hour, 50μM of benzyloxycarbonyl FY(*t*-Bu)-DMK, an irreversible, highly specific inhibitor of cathepsin L (Sigma # 219427) was added to quench cathepsin L activity. Once activated, cathepsin A and C were used in the experiments outlined. Similarly, for cathepsin H activation, 1μM of cathepsin H was incubated with 500nM of Thermolysin (R&D # 3097-ZN) at room temperature for 3 hours. After 3 hours, 1mM of Phosphoramidon (Tocris # 6333), a specific thermolysin inhibitor, was added to quench Thermolysin activity. Once activated, cathepsin H was used in the experiments outlined. To confirm each protease was enzymatically active, protease activity control experiments were performed using a FRET-based fluorogenically labeled casein assay (Biovision #K781), according to the vendor's protocol. In brief, 1μM of each protease was added to a 50μL reaction mixture using the recommended concentration of control fluorogenic substrate in a buffer consisting of 50mM sodium acetate buffer at pH 4.5 and in the presence of 1mM EDTA and 2mM DTT. The assay was performed at 37ºC for 60 minutes and readings were taken every 2 minutes using Tecan Infinite M Plex plate reader.

Statistical analysis

Details of the statistical test used for each experiment is in figure legends along with n number and *p* value. All data is represented as mean ± SD. Statistical analysis was performed using GraphPad Prism 8 (GraphPad Software, La Jolla, California USA). A *P*-value < 0.05 was considered significant.

Cell culture, treatment, and lysis

Cell culture - SH-SY5Y human neuroblastoma cells were obtained from ATCC (CRL-2266) and maintained 1:1 EMEM/F12 media (ATCC #30-2003/Thermo #11765062) supplemented with 10% FBS and 1% Penicillin-Streptomycin (Thermo #15140122). SH-SY5Y cells were differentiated by treating with 10μM all-trans retinoic acid (Sigma #R2625) for 6 days in EMEM/F12 media supplemented with 10% FBS and 1% Penicillin-Streptomycin, followed by 4 days of treatment with 50ng/mL of BDNF (Peprotech #450-02B) in EMEM/F12 media supplemented with only 1% Penicillin-Streptomycin. HEK293FT were maintained in high glucose DMEM media with 10%FBS and 1% Penicillin-Streptomycin.

Cell treatments - For protease inhibition studies, day 10 post-differentiation SH-SY5Y cells were treated with 10μM E64D (Tocris Bioscience #4545), 20μM cathepsin L inhibitor II (Santa Cruz #sc-3132), and 15μM of CA074_methyl ester (Caymen Chemical Company #18469) or DMSO for 24 hours. For siRNA studies, day 10 post-differentiation SH-SY5Y cells were transfected according to the manufacturer's protocol using Oligofectamine (Invitrogen #12252011). Sixty hours post transfection, cells were collected for western blot analysis, as described below. siRNA scramble (Thermo Fisher #4390843), siRNA Legumain (Santa Cruz #sc-60930) were used. For overexpression studies, pCMV6 mammalian expressing vectors carrying the cDNA of AEP were ordered from Origene (#RC224975). XtremeGene HP (Sigma, # 06366236001) was used to transiently transfect HEK293FT cells for 24hours following the manufactures suggestions. The cells were then pelleted and prepared for western blotting as described below.

Cell Lysis - The cells were collected post-treatment and prepared for western blot analysis. Cells were washed once with PBS, trypsinized, and pelleted. The pellets were lysed in RIPA buffer (Fisher #89900) with protease and phosphatase inhibitors (Sigma #4693124001, #4906837001) and centrifuged at 15000 rpm at 4ºC for 20 minutes. The supernatant containing the soluble proteins were transferred into a new tube. Estimated protein concentration with a Peirce BCA (Fisher # PI23225) protein assay kit following manufacturer's instructions. The nitrocellulose membrane was blocked with 5% milk (Fisher #NC9121673) or Odyssey buffer (Li-cor #927-50010) for 1-2hrs. The membranes were cut between 60-50kD and between 20-15kD to obtain PGRN and granulin-specific bands respectively and incubated with primary antibodies overnight [19]. Li-cor secondary antibodies at 1:5000 dilution was used and imaged using Odyssey CLx imager. Western blots were quantified using FIJI software.

Cloning CRISPR guide and Viral packaging

Using a protocol similar to Sanjana et, 2014, CRISPR guide (sgRNA), GGTCCAGGCAGCAGGCCACAGGG targeting the PGRN gene was cloned into pLentiV2 (Addgene, #52961) at the BsmBI site and confirmed by sequencing [22]. For viral production, $3x10^6$ HEK293FT cells were seeded in a 10cm dish. 24 hours post seeding, cells were transfected with either pLentiV2 with guide sequence or only the backbone (mock), psPax2 (Addgene, #12260) and pCMV- VSV-G (Addgene, #8454) using XtremeGene HP (Sigma, # 06366236001) following manufacturer's guidelines. 12-16 hours post transfection, fresh media was added. 48 hours post transfection, virus containing media was collected and filtered using a 0.45μM syringe filter.

Generation of PGRN knock-out SH-SY5Y line

To generate a PGRN KO, Human SH-SY5Y cells were infected with the virus and polybrene (4μg/mL) in 6 well plates. 24 hours post infection, cells were selected using 1μg/mL puromycin. To select the PGRN KO SY-SY5Y cells, single clones were isolated and genomic DNA from each clonal population was extracted with the QuickExtract kit (Epicentre). The region of interest was amplified from genomic DNA by PCR using primers (forward -TGTAAAACGACGGCCAGTGGGCTAGGGTACTGAGTGAC

and reverse -CAGGAAACAGCTATGACCCTGATGGCACGCTCACCTCT) and sequenced to determine the mutation. Cell lysates from each clone was extracted (see below) and PGRN and granulin levels were determined by western blots. With this method, a successful KO clone was identified and validated. These cells were then expanded and frozen for the experiments outlined.

Antibodies

Antibody generation - The following epitopes were used to generate the rabbit polyclonal anti-bodies:

paragranulin (p-Gran) -TRCPDGQFCPVACCLDPGGASYSCCRPLLD,

granulin F (Gran-F) - QCPDSQFECPDEST, and

granulin E (Gran-E) - ECGEGHFCHDNQTCCR.

Antibody validation – The sensitivity, specificity, and reproducibility of results of the novel p-Gran, Gran-F, and Gran-E antibodies were validated using a protocol similar to Bordeaux, et al. 2010 [23]. In brief, antibody specificity for each antigen was first measured by dot blot. For these experiments, 2.5µg of each granulin peptide was pipetted onto a nitrocellulose membrane defined into grids. Each antibody was incubated with the membrane overnight at 1:1000 dilution. Signals from the primary antibodies were amplified using species-specific antisera conjugated with horseradish peroxidase (Cell Signaling #7074) and detected with a chemiluminescent substrate detection system ECL and scanned the images with a densitometer. Following successful confirmation of antibody sensitivity, the specificity was evaluated via a peptide blocking experiment. Recombinant human progranulin was incubated with CTSL, a known PGRN protease, at pH 4.5 for 20 minutes at 37C as previously described. Samples were denatured and western blots were performed for peptide blocking analysis. Each primary antibody (p-Gran, Gran-F, Gran-E) was pre-incubated with its respective granulin peptide for 2 hours at room temperature with gentle mixing. Each primary antibody (p-Gran, Gran-F, Gran-E) was pre-incubated with its respective granulin peptide for 2 hours at room temperature with gentle mixing. Optimal primary antibody concentration was incubated with two different peptide amounts and on its own. Primary antibody to peptide ratio was determined by molarity at 10X, 100X, and no peptide. Following incubation, solutions were used to blot membranes overnight at 4C. Normal western blot procedure was completed as described.

Commercial antibodies - Anti-progranulin C-terminus (Thermo Fisher #40-3400, 1:200), Anti-granulin F (Sigma #HPA008763, 1:250), Anti-AEP (R&D #AF2199, 1:500), anti-Actin (Sigma #MAB1501R, 1:5000), and anti-FLAG (Sigma #F3165)

Human brain tissue lysis and analysis

Brain tissue was prepared as previously described in Salazar et al, 2015 [12]. Briefly, adjacent tissue blocks were fixed, embedded in paraffin wax, sectioned, stained for hematoxylin and eosin, and rated for astrogliosis (0–3 scale). Absent or low gliosis regions were selected with a score of 0-1, while high levels of gliosis regions with a score of 2-3. From this, we selected the middle frontal gyrus (MFG) with severe

degeneration and inferior occipital cortex (IOC) with no degeneration for all assays. The same region was collected from control subjects. Brain tissue samples were weighed, diluted 25-fold with PBS (Thermo Fisher #14190250) and 1% triton-X (Millipore Sigma, #T9284), homogenized for 1 minute (pestle pellet motor) and sonicated for 5 rounds of 30 seconds on and 1 minute off (BioRuptor, Diagenode). The lysate was centrifuged at max for 20 minutes and the soluble supernatant was used for western blot assays. BCA was performed to determine protein concentration according to manufacturer's instructions. 25µg of total protein from each sample was loaded for western blot analysis. The nitrocellulose membrane was blocked with 5% milk (Fisher #NC9121673) or Odyssey buffer (Li-cor, #927-50010) for 1-2hrs. The membranes were cut between 60-50kD and between 20-15kD to obtain PGRN and granulin-specific bands respectively and incubated with primary antibodies overnight [19]. Li-cor secondary antibodies at 1:5000 dilution was used and imaged using Odyssey CLx imager. Western blots were quantified using FIJI software.

qPCR

Differentiated SH-SY5Y cells were pelleted and RNA was extracted using standard phenol:chloroform extraction techniques. 1µg of RNA was reverse transcribed to cDNA using Superscript III reverse transcription kit following manufacturer's protocol (Thermo Fisher #18080044), random primers (Thermo Fisher #48190011) and dNTPs (Sigma #11969064001). RT-qPCR was performed using TaqMan Fast Advanced Master Mix (Thermo Fisher #4444557) in a ABI Prism 7900HT Sequence Detection System (Applied Biosystems), with TaqMan FAM probes for human CTSB (Hs00947433_m1), CTSL (Hs009964650_m1), CTSK (Hs00166156_m1), CTSS (Hs00175407_m1), AEP/LGMN (Hs00271599_m1), CTSV (Hs00426731_m1), CTSE (Hs00157213_m1), CTSG (Hs01113415_g1) and the house keeping gene GAPDH (Hs02758991_g1) as a control. Four biological samples were analyzed, each with three technical replicates. mRNA levels of target genes were normalized to the mean of the house keeping gene GAPDH. Data is displayed as relative values compared to GAPDH.

Enzyme activity assays

AEP activity assay - AEP substrate Z-Ala-Ala-Asn-AMC (Bachem #I1865) was used to measure activity. 50mM sodium acetate buffer pH 5.5 with 2mM DTT, 1mM EDTA and 0.1% CHAPS was used as the assay buffer. 100µM of the substrate was used per reaction. The assay was performed at 37ºC for 60 minutes and readings were taken every 2 minutes using Tecan Infinite M Plex plate reader. Activity was measured using excitation wavelength 380nm and emission wavelength 460nm. Assays were performed in triplicates for each sample.

CTSL activity assay - Biovision CTSL fluorometric assay kit (#K142) was used according to manufacturer's protocol with some modifications. Since CTSB can also cleave the assay substrate, the assay was performed with 1mM CTSB inhibitor (CA074_ME, Caymen Chemical Company #18469) to specifically assay CTSL activity. The assay was performed at 37ºC for 60 minutes and reading were taken every 2 minutes using a Tecan Infinite M Plex plate reader. Activity was measured using excitation

wavelength 400nm and emission wavelength 505nm. This assay was performed in triplicates for each sample.

Identification of AEP cleavage sites

In-gel Digestion - 400 ng of recombinant human progranulin (R&D #CF-2420) was incubated at 37ºC for 60 minutes with recombinant human AEP (R&D #2199-CY) at pH 4.5. The cleavage was stopped by adding 7.5µl of NuPAGE 4X LDS (Fisher #NP0007), 3µl of 10X reducing agent (Fisher #NP0009) and denatured for 10 minutes at 70ºC. The samples were run on precast NOVEX 4-12% Bis-Tris gels (Fisher #NP0321PK2) using MES buffer (Fisher #NP0002). The gel was fixed, and silver stained as described above. Protein bands were excised and digested in-gel with Endoproteinase Asp-N (Sigma-Aldrich #11054589001) as described previously [24, 25]. The extracted digests were vacuum-evaporated, resuspended in 20µl of 0.1% formic acid, and desalted using C18 ZipTips (Millipore #ZTC18M096).

Mass Spectrometry - Asp-N peptides were analyzed by on-line LC-MS/MS using an Orbitrap Fusion Lumos (Thermo Scientific, San Jose, CA) coupled with a NanoAcquity M-Class UPLC system (Waters, Milford, MA). Peptides were separated over a 15cm x 75µm ID 3µm C18 EASY-Spray column (Thermo Scientific #ES800). Precursor ions were measured from 375 to 1500 m/z in the Orbitrap analyzer (resolution: 120,000; AGC: 4.0e5). Ions charged 2+ to 7+ were isolated in the quadrupole (selection window: 1.6 m/z units; dynamic exclusion window: 30 s; MIPS Peptide filter enabled), fragmented by HCD (Normalized Collision Energy: 30%) and measured in the Orbitrap (resolution: 30,000; AGC; 5.0e4). The cycle time was 3 seconds.

Peaklists were generated using PAVA (UCSF) and searched using Protein Prospector 5.23.0 against the SwissProt database (downloaded 9/6/2016) and a randomized concatenated database. Cleavage specificity was set as Asp-N/AEP (Asn-C) allowing 2 mis-cleavages. Carbamidomethylation of Cys was set as a constant modification and two of the following variable modifications were allowed per peptide: acetylation of protein N-termini, oxidation of Met, oxidation and acetylation of protein N-terminal Met, cyclization of N-terminal Gln, protein N-terminal Met loss, protein N-terminal Met loss and acetylation. Precursor mass tolerance was 20ppm and fragment mass tolerance was 30ppm. A subsequent search using the above parameters but limiting the search to the following accession numbers and a user defined PGRN amino acid sequence (the human sequence minus the first 18 amino acids and with a C-terminal 6xHis tag) was used for further analysis: B2FQP3 O08692 P02533 P02666 P02754 P02769 P04264 P28799 P35527 P35908 P85945 Q8PC00 Q91FI1 Q9R4J4 P07711 Q99538. Spectra containing AEP cleavage sites can be viewed in MS-Viewer with the search key “besr1qb6q4” or the following link: http://msviewer.ucsf.edu/prospector/cgi-bin/mssearch.cgi?report_title=MS-Viewer&search_key=besr1qb6q4&search_name=msviewer [26].

Results

Multiple lysosomal proteases digest human progranulin *in vitro*

Previous studies have identified CTSL and CTSB as intracellular PGRN proteases [17,19], however the endo-lysosomal compartment contains several classes of proteolytic enzymes with specific but overlapping peptide recognition motifs [26]. Thus, we posited that other lysosomal enzymes may also play a role in processing human PGRN. To identify which proteases can and cannot cleave PGRN, we performed an extensive *in vitro* cleavage study with commercially available recombinant human lysosomal enzymes. Most of these enzymes were purchased in their active form or can undergo auto-activation. However, some of these enzymes required activation. Since different proteases have distinct pH setpoints for optimal activity that can be substrate-dependent [27-29], we performed the study across a range of pH settings that represents the stepwise maturation of endo-lysosomal compartments. Although we were ultimately interested in which of the proteases can liberate individual granulin peptides, we first asked the question of which lysosomal proteases can *digest* or *break down* the full-length pro-protein in the inter-granulin linker regions (Figure 1a).

Lysosomal proteases are classified based on the amino acid(s) in their active site cleft. We first assayed the largest class of lysosomal proteases, the cysteine protease family [30,31]. We visualized our results by separating the proteins on a poly-acrylamide gel and silver staining (Figure 1b). As previously shown, the cysteine proteases CTSB and CTSL were able to digest recombinant human PGRN. In addition, cathepsins K (CTSK), S (CTSS), V (CTSV) and asparagine endopeptidase (AEP) were also able to digest PGRN within 20 minutes. At an acidic pH of 4.5 or 5.5, CTSB, CTSL, CTSK, CTSS and CTSV digested most or all of full-length PGRN. AEP only modestly digested PGRN at pH 4.5 and 5.5 within the same time frame. CTSL and CTSV (also known as cathepsin L2), digested PGRN at pH as low as 3.4. Interestingly, CTSS, a lysosomal and secreted enzyme, is the only cysteine protease that can efficiently digest PGRN at both acidic and neutral pH, thereby making it a candidate enzyme to process both intracellular and extracellular PGRN [32]. In contrast, the cysteine cathepsins H (CTSH), C (CTSC), F (CSTF), O (CTSO) and X (CTSX) were unable to digest PGRN at any pH tested (Fig. 1b).

We next tested the aspartic acid family of acid hydrolases, which includes cathepsin E (CTSE), cathepsin D (CTSD) and napsin A. Cathepsin E (CTSE) is an endo-lysosomal aspartyl protease, highly expressed in immune cells such as microglia [33]. CTSE digested PGRN only at very acidic pH (Fig. 1c). CTSD has also been implicated in multiple neurodegenerative diseases and was previously demonstrated to associate with PGRN, affecting both CTSD levels and activity [14, 34-39]. One recent study reported that prolonged incubation (16 hours) of PGRN with CTSD at pH 3.5 can lead to PGRN cleavage, although low molecular weight granulin-sized bands were not observed [20]. Typically, proteases act on their substrates rapidly, within minutes. To determine if CTSD plays a role in degrading PGRN at more physiological time scales, we incubated mature CTSD with recombinant PGRN for 20 minutes. Under these *in vitro* conditions, CTSD did not degrade PGRN (Fig. 1c). To ensure that CTSD was indeed active, we tested its activity against a known substrate, BSA [40], in parallel with PGRN. At both pH 3.4 and 4.5, CTSD cleaved BSA but not PGRN (Fig. S1a). Thus, PGRN is likely not a physiological CTSD substrate or if it is, its activity is slow and limited. Napsin A, which has been used as a biomarker of human cancers [41,42], did not degrade PGRN *in vitro* at any pH tested (Fig. 1c).

We then tested the final class of lysosomal proteases, the serine proteases cathepsin G (CTSG), pro-X-carboxypeptidase (PRCP) and cathepsin A (CTSA). PRCP and CTSA were unable to digest PGRN at any pH tested. However, CTSG, a lysosomal and secreted serine protease digested PGRN at pH 5.5 and 7.4 (Fig. 1d). Therefore, CTSG is another candidate protease that may process both intracellular and extracellular PGRN.

To determine if the enzymes that do not cleave PGRN in our assay (CTSH, CTSC, CTSF, CTSO, CTSX, CTSD, napsin A, PRCP and CTSA) are active against another control substrate, we performed FRET-based cleavage assays with fluorogenically-tagged casein. The results confirm that all enzymes are active at pH 4.5 and can cleave this universal substrate (Fig. S1b).

Therefore, in total six cysteine (CTSB, CTSL, CTSK, CTSS, CTSV and AEP), one aspartyl (CTSE) and one serine protease (CTSG) rapidly digested full-length PGRN *in vitro* at varying pH settings (Fig. 3a and Table 1). Since protease expression can be temporal and cell-type specific [27,43,44], these results suggest that PGRN processing may occur in a protease-specific, pH-dependent manner and possibly both outside and in multiple compartments within the cell.

PGRN undergoes pH-dependent processing into multi-granulin fragments and individual granulins *in vitro*

Progranulin is well-known to be a precursor protein for granulins, which are stress-responsive molecules with varying bioactivities [6-10]. Having established a subset of lysosomal proteases that can digest full-length PGRN, we next sought to understand which of these could proteolytically process PGRN into granulin-sized peptides. To do so, we generated anti-granulin antibodies raised against the N-terminal paragranulin (p-Gran), a centrally located peptide, granulin F (Gran-F), and C-terminal granulin E (Gran-E) (Fig. 2a and S2) and performed western blot analysis to assess the results of *in vitro* cleavage assays. Consistent with our previous results, the lysosomal proteases that could not digest PGRN did not release any specific multi-granulin or individual granulin-sized fragments (Fig. S3). Somewhat to our surprise, we found that each of the enzymes that could digest PGRN was able to process it into distinct multi-granulin fragments and individual granulin peptides. Moreover, this processing was pH dependent (Fig. 2 and S4).

The N-terminal paragranulin can be released by a cleavage between granulins p and G, and we detected this activity for CTSL and CTSK, and to a lesser extent in CTSS and CTSV (Fig. 2b and S4). Similarly, the C-terminal granulin E can be released by a cleavage between granulins D and E, and we detected this activity for CTSL, CTSK, and CTSV, and to a lesser extent CTSB, CTSS and CTSG (Fig. 2d and S4). Interestingly, the endo-lysosomal aspartyl protease CTSE also had the ability to process PGRN to release an ~12kD peptide containing granulin E, but only at pH 3.4, suggesting that CTSE may have a different cleavage pattern than other proteases (Fig. 2d). Unlike paragranulin and granulin E, the release of granulin F requires two cleavages, one between granulins G-F and one between granulins F-B. Most individual proteases were inefficient at cleaving these specific linkers. CTSL, CTSK, CTSS and CTV robustly cleaved PGRN into multi-granulin containing granulin F, but inefficiently released very small amounts of individual granulin F only at pH 4.5 (Fig. 2c). Contrastingly, AEP, which robustly released granulin F at pH 4.5 and 5.5, was a notable exception. However, AEP was unable to liberate the N and C-

terminal granulins (Fig. 2c and S4). These results suggest that different proteases cleave at different inter-granulin regions in PGRN.

Given that each intact PGRN molecule contains up to eight granulins and seven inter-granulin linkers, the potential number of different multi-granulin fragments could be quite high (~86 reactions). However, when we observed the actual pattern of multi-granulin fragments, we found that their molecular weights were largely similar across both cysteine and serine proteases. This suggests similar cleavage patterns for the different enzymes, albeit with different abundances (Fig. 2). Interesting differences also emerged across acidic pH, including shifts in the size of multi-granulin and individual granulin-sized bands (Fig. 2). The notable exception to this pattern, once again, was AEP, which exhibited a distinctive pattern of intermediate bands.

In summary, our results demonstrate that eight lysosomal proteases are capable of digesting full-length human PGRN *in vitro*. Moreover, these findings demonstrate that each of these enzymes can cleave PGRN into one or more granulin (Fig. 3b). When tested in isolation, the majority of cysteine, aspartyl and serine proteases tended to liberate N and/or C-terminal granulins. In contrast, AEP was unable to liberate the N- and/or C-terminal granulins but robustly liberated granulin F, present in the center of the pro-protein. Furthermore, one cysteine (CTSS) and one serine protease (CTSG) processed PGRN into granulins at neutral pH (7.4) while an aspartyl protease (CTSE) could only process PGRN at highly acidic pH (3.4).

Asparagine endopeptidase is a PGRN protease that liberates granulin F

To study the processing of endogenous PGRN in cells, we assessed the specificity of our in-house anti-granulin antibodies using a PGRN knockout (KO) neuroblastoma cell line we generated using CRISPR/Cas9-based gene editing (Fig. S5-6). Although our antibodies showed specificity *in vitro*, they were unable to recognize full-length PGRN or individual granulins from whole cell lysates, possibly due to epitope blocking by post-translational modifications (Fig. S3 and S6a). A recent study of all available commercial PGRN antibodies showed that only endogenous granulin F can be reliably detected in cell lysates from multiple cell type, using an antibody from *Sigma* [19]. The widely used *Invitrogen* antibody reliably detects full length progranulin in differentiated SH-SY5Y cells, however, it does not detect any granulin sized bands in whole cell lysates (Fig. S6). In contrast, the *Sigma* antibody, can detect a granulin sized band (Gran-F) but cannot be used to detect full-length PGRN in whole cell lysates (Fig. S6). Therefore, we utilized these two commercial antibodies to study to detect both PGRN and granulin F in our cellular studies. Terminally differentiated SH-SY5Y neuroblastoma cells endogenously produce detectable amounts of both PGRN and granulin F (Fig. S5). Therefore, we used these neuron-like cells to determine the expression profile of the candidate PGRN proteases by qPCR analysis. We found that the lysosomal proteases CTSB, CTSL, CTSK, CTSS, AEP and CTSE were expressed in differentiated SH-SY5Y cells, but CTSV and CTSG were not detected (Fig. S7). Of the expressed proteases, AEP is the only one that robustly liberates granulin F *in vitro*. Since granulin F is the only granulin that can be reliably detected from cell lysates, we sought to further validate AEP as a PGRN protease in these cells [19].

To determine if AEP cleaves PGRN endogenously in terminally differentiated SH-SY5Y cells, we performed both an siRNA knock down of AEP and assessed the levels of endogenous PGRN and granulin F in terminally differentiated SH-SY5Y cells. Consistent with our *in vitro* results, a moderate knock down of AEP resulted in a significant decrease in the levels of granulin F compared to scramble-treated controls, implicating AEP as a PGRN protease that liberates granulin F in this cell model (Fig. 4a). To further validate our results, we transiently overexpressed FLAG-tagged AEP in HEK293FT cells (Fig. 4b). Overexpression of AEP lead to significant increase in granulin F levels with a moderate decrease in full length PGRN compared to mock controls implicating AEP as a PGRN protease (Fig. 4b). Interestingly, knockdown of AEP did not affect the levels of full-length PGRN compared to scramble-treated cells (Fig. 4a).

To determine which other candidate proteases expressed in these cells could affect the levels of endogenous PGRN and granulin F, we used cell-permeable protease inhibitors that inhibit all cysteine proteases (except AEP) [8] and known PGRN proteases, CTSB and CTSL [20]. Unlike knockdown of AEP, protease inhibition led to an increase in full-length PGRN in all conditions, reaching significance when both CTSB and CTSL are inhibited compared to vehicle-treated controls (Fig. 4c). This reinforces that both CTSB and CTSL can process full-length PGRN *in vivo*. To determine if the increase in PGRN levels affected granulin F production, we assessed the levels of granulin F upon CTSB and CTSL protease inhibition. Individual CTSB or CTSL inhibition did not significantly change levels of granulin F, with only a modest decrease upon inhibition of both proteases (Fig. 4c). These data are consistent with the *in vitro* studies where both CTSB and CTSL processed PGRN into multi-granulin fragments but were inefficient at releasing granulin F compared to AEP (Fig. 2c). This data suggests that in cells, endogenous AEP likely liberates granulin F from an existing multi-granulin fragment produced by another cysteine protease, possibly CTSB and/or CTSL, that is able to process full-length PGRN (Fig. 2).

To determine the specific cleavage sites of AEP, we incubated recombinant human PGRN with and without AEP for 60 minutes at pH 4.5. Bands corresponding to full-length, uncleaved PGRN, multi-granulin bands, and granulin-sized bands were observed by silver staining (Fig. S8a). All bands underwent LC-MS/MS to determine AEP cleavage sites. Consistent with its activity as a protease that cleaves after asparagine residues, we identified four sites for AEP cleavage within three inter-granulin linkers (G-F, F-B, B-A) that would result in the liberation of granulins F and B from PGRN (Fig. 5, S8b-S8e).

Granulins F levels are increased in the degenerating regions of the brains from FTLD-TDP-*Pgrn* patients

PGRN haploinsufficiency leads to FTLD. Interestingly, in *C. elegans*, the processing of progranulin to granulins increases with age [45]. Further, the presence of an MGF containing gran E is decreased in FTLD-TDP [12]. However, whether PGRN processing into individual granulins is affected in FTLD, an age-related disorder, is unclear. To assess whether PGRN processing is altered in FTLD, we measured granulin F levels from brain samples of control individuals or those with FTLD due to *Pgrn* mutations (FTLD-TDP-*Pgrn)*. As previously described [12], we examined a brain region affected in FTLD (middle frontal gyrus,

MFG, defined as gliosis score of 3) as well as an unaffected region (inferior occipital cortex, IOC, defined as gliosis score of 0) from both groups. Characteristics of subjects are shown in Table 2.

Similar to previous studies [19, 46], the FTLD-TDP-*Pgrn* group exhibited significantly less full-length PGRN protein in both unaffected and affected brain regions compared to control subjects (Fig. 6a and 6b). Interestingly, however, granulin F was increased relative to controls in the diseased MFG region (Fig. 6a and 6c). Since AEP was the only enzyme that could robustly liberate granulin F in our *in vitro* assay and affected the levels of granulin F in cells (Fig. 3 and 4), we quantified the levels of AEP in both regions of the brain. We found a significant increase in the levels of mature-AEP in the degenerating MFG regions compared to non-degenerating IOC regions in FTLD-TDP-*Pgrn* patients (Fig. 6d and S9). Furthermore, activity assays revealed an increase in AEP activity in disease-affected MFG compared to non-affected IOC from the same subjects, as well as a trend toward increased activity ($p=0.07$) in FTLD-Pgrn IOC versus MFG (Fig 6e). However, no difference was found in AEP activity between FTLD-TDP-*Pgrn* and control subjects in the IOC. To determine if the change in levels and activity AEP was also seen for other PGRN proteases, we assayed the activity of CTSL, a previously known PGRN protease. Interestingly, there was no significant change to CTSL activity in either region across groups, suggesting differential effects on lysosomal enzymes in FTLD (Fig. 6f).

These data are all consistent with a model in which increased AEP activity in the degenerating MFG region alters PGRN processing in a way that leads to an increase in production of granulin F in that region. We were unable to detect other granulin peptides but had previously shown in both FTLD-TDP patients negative for *Pgrn* mutations and Alzheimer's disease brain that a multi-granulin fragment containing granulin E was also increased in a diseased brain region [12]. Thus, it may be that either these neurodegenerative diseases or the gliosis associated with them leads to overall increased processing of PGRN.

Discussion

In this study, we sought to identify the molecular players involved in liberating individual granulins from PGRN, which may ultimately aid in better understanding of granulin function in health and disease. These studies revealed that multiple proteases can process PGRN and liberate granulins in a pH-dependent manner. Although these proteases have a known pH range of activity, the precise pH optima may be substrate dependent. For example, cathepsin D optimally degrades actin at pH 4 while for tubulin the pH optima is slightly above pH 5 [28]. As such, we chose to survey PGRN at range of pHs to determine the pH optima of the proteases on PGRN specifically.

Additionally, these proteases are reported to have differential expressions in cells and tissues. CTSB, CTSL and AEP are expressed in all cells and tissues including the brain, however CTSS, CTSK, CTSV, CTSE and CTSG show cell and tissue specific-expression [2,31,43,44]. This suggests that PGRN processing may be regulated in a cell-type specific manner and future studies in cells that endogenously express these proteases may help better understand their roles.

Although our *in vitro* assays identified the ability of individual proteases to cleave PGRN into granulins, we recognize that in lysosomes, many proteases may be acting simultaneously [47]. The experiments in terminally differentiated SH-SY5Y cells revealed that individual granulins may be produced by serial or stepwise cleavage of PGRN by multiple proteases. These results suggest that cysteine proteases such as CTSB and/or CTSL process full-length PGRN to mainly produce multi-granulin fragments that contain granulin F and to a lesser extent individual granulin F (similar to our *in vitro* assay), while AEP may act on one or more of these fragments to produce individual granulin F. It is therefore possible that the modest reduction in granulin F levels seen upon dual inhibition of CTSB and CTSL is due to reduced availability of multi-granulin fragments for AEP to process. To our knowledge, this is the first study to identify cleavage sites in the inter-granulin linkers required to liberate granulin F. Earlier studies in human primary cell cultures have also referred to a potential multi-granulin fragment likely containing granulin F [48,49]. Future studies on these multi-granulin fragments will be essential to tease out the complex regulation of PGRN processing.

While we and others have shown alterations in granulin levels in FTLD-TDP [12, 19], this study is the first study to implicate a change in a specific protease, AEP. To our surprise, these results also demonstrated elevated granulin F levels in areas of severe neurodegeneration in human GRN-FTD cases. Previously, Holler et al, 2017, demonstrated a reduction in certain granulins in brain, however, the severity of degeneration and astrogliosis within these regions was not assessed [19]. Since these degenerating regions are characterized by neuronal loss and infiltration of inflammatory astrocytes and microglia, the latter of which expresses high levels of AEP [49], it is possible that gliotic cells are responsible for the increased granulin F. Moreover, since PGRN is also a secreted protein we cannot yet differentiate the cell autonomous and cell non-autonomous contributions of PGRN processing in disease. Whether the increased granulin F contributes to or results from FTLD pathophysiology also remains to be seen. AEP has previously been reported to cleave aggregate-forming proteins, such as amyloid precursor protein (APP), microtubule associated protein tau (MAPT) and TAR-DNA binding protein 43 (TDP43) and is also implicated in an FTLD-related disorder, amyotrophic lateral sclerosis (ALS) [31,50-53]. Interestingly, AEP is dysregulated and activated during aging, and AEP activity is increased in regions of degeneration in AD human brain and mouse models suggesting that PGRN processing and granulin F production may be altered in other neurodegenerative diseases as well [51]. If future studies implicate a causal role for granulin F in FTLD and other diseases, targeting AEP to decrease the levels of granulin F in the degenerating regions of the brain may be neuroprotective.

In summary, our study suggests that PGRN processing into granulins undergoes multiple levels of regulation, including protease-specific cleavage sites in the various inter-granulin linkers and differential cleavage based on pH setpoints, which may reflect activity in different endo-lysosomal compartments. Still to be explored are cell-type and temporal regulation of PGRN cleavage. Given the highly evolutionarily conserved presence of PGRN and granulins, as well as the gene mutations associated with disease, intricate regulation indicates that PGRN and granulin levels are important for maintaining cellular homeostasis and function. Our studies have helped identify multiple players that contribute to

this homeostasis, providing new avenues to regulate the levels of granulins in disease and placing the broad and contrasting roles of granulins into perspective.

Conclusion

This study comprehensively identifies a suite of endo-lysosomal proteases that can process full-length PGRN into multi-granulin and single granulin fragments. These proteases have strikingly specific cleavage patterns and optimal pH settings. The complexity of PGRN cleavage could confer multiple layers of cell-type and environmentally responsive regulation upon PGRN processing that can be altered with age and disease. As full-length, multi-granulin and single granulin fragments likely have different biological activities, these findings are highly relevant in understanding the consequences of progranulin replacement therapies and could be leveraged to promote neuronal health through inhibition of specific PGRN proteases.

Declarations

Ethical Approval and consent to participate

Not Applicable

Consent of publication

All authors have reviewed the final manuscript and consent to publication.

Availability of supporting data

Additional data is available online.

Completing interests

The authors declare they have no completing interests.

Funding

This work was supported by National Institute of Health R01NS095257 and R01AG059052. We also thank The Paul G. Allen Family Foundation for research support. Human tissue samples were provided by the Neurodegenerative Disease Brain Bank at the University of California, San Francisco, which receives funding support from NIH grants P01AG019724 and P50AG023501, the Consortium for Frontotemporal Dementia Research, and the Tau Consortium. The mass spectrometry results were supported by a grant from the Adelson Medical Research Foundation. The Thermo Scientific Fusion Lumos was funded by the UCSF Program for Breakthrough Biomedical Research (PBBR).

Author contributions

S.M and A.W.K conceived the project. S.M designed all experiments. P.J.S. and E.C.C. performed many of the *in vitro* western blots and silver stain experiments as well as the enzyme activity assays. A.P assisted in knock down and over-expression studies. K.H.L, J.C.M and A.B. performed LC/MS/MS. A.M performed the dot blot analysis. W.W.S. and B.L.M. provided the brain samples. A.R.A performed the peptide blocking assay and the brain western blots. S.M performed all other experiments and analyzed all the data. S.M, P.J.S. and A.W.K wrote the manuscript.

Acknowledgements

We would like to thank Alissa Nana Li and Celica Cosme and the UCSF Neurodegenerative Disease Brain Bank for providing human brain tissue samples. Human tissue samples were provided by the Neurodegenerative Disease Brain Bank at the University of California, San Francisco, which receives funding support from NIH grants P01AG019724 and P50AG023501, the Consortium for Frontotemporal Dementia Research, and the Tau Consortium. We would like to thank Imani Robinson for help with sample preparations. We thank all members of the Kao lab for helpful discussions.

Authors' information

Not Applicable

Abbreviations

PGRN - Progranulin

Gran-F – granulin F

p-Gran – paragranulin

Gran-E – granulin E

CTSB – Cathepsin B

CTSL – Cathepsin L

CTSK – Cathepsin K

CTSS – Cathepsin S

CTSV – Cathepsin V

AEP – Asparagine endopeptidase

CTSH – Cathepsin H

CTSX – Cathepsin X

CTSC – Cathepsin C

CTSD – Cathepsin D

CTSE – Cathepsin E

CTSF – Cathepsin F

CTSO – Cathepsin O

CTSG – Cathepsin G

PRCP – Pro-X carboxypeptidase

CTSA – Cathepsin A

FTLD-TDP-*Pgrn* – Frontotemporal lobar degeneration leading to TDP-43 positive inclusions caused by progranulin haploinsufficiency

AD – Alzheimer's disease

MAPT -microtubule associated protein Tau

IOC – inferior occipital cortex

MFG – middle frontal gyrus

References

1. Kao AW, McKay A, Singh PP, Brunet A, Huang EJ. Progranulin, lysosomal regulation and neurodegenerative disease. Nat Rev Neurosci. 2017;18:325–33.
2. Palfree RGE, Bennett HPJ, Bateman A. The Evolution of the Secreted Regulatory Protein Progranulin. Robinson-Rechavi M, editor. PLoS ONE. 2015;10: e0133749.
3. Baker M, Mackenzie IR, Pickering-Brown SM, Gass J, Rademakers R, Lindholm C, et al. Mutations in progranulin cause tau-negative frontotemporal dementia linked to chromosome 17. Nature. 2006;442:916–9.
4. Cruts M, Gijselinck I, Van der Zee J, Engelborghs S, Wils H, Pirici D, et al. Null mutations in progranulin cause ubiquitin-positive frontotemporal dementia linked to chromosome 17q21. Nature. 2006;442:920–4.
5. Smith KR, Damiano J, Franceschetti S, Carpenter S, Canafoglia L, Morbin M, et al. Strikingly Different Clinicopathological Phenotypes Determined by Progranulin-Mutation Dosage. The American Journal of Human Genetics. The American Society of Human Genetics; 2012; 90:1102–7.

6. Kessenbrock K, Fröhlich L, Sixt M, Lämmermann T, Pfister H, Bateman A, et al. Proteinase 3 and neutrophil elastase enhance inflammation in mice by inactivating antiinflammatory progranulin. J Clin Invest. 2008;93:849.
7. Tang W, Lu Y, Tian QY, Zhang Y, Guo FJ, Liu GY, et al. The Growth Factor Progranulin Binds to TNF Receptors and Is Therapeutic Against Inflammatory Arthritis in Mice. Science. 2011;332:478–84.
8. Zhu J, Nathan C, Jin W, Sim D, Ashcroft GS, Wahl SM, et al. Conversion of proepithelin to epithelins: roles of SLPI and elastase in host defense and wound repair. Cell. 2002;111:867–78.
9. Tolkatchev D, Malik S, Vinogradova A, Wang P, Chen Z, Xu P, et al. Structure dissection of human progranulin identifies well-folded granulin/epithelin modules with unique functional activities. Protein Sci. 2008;17:711–24.
10. Plowman GD, Green JM, Neubauer MG, Buckley SD, McDonald VL, Todaro GJ, et al. The epithelin precursor encodes two proteins with opposing activities on epithelial cell growth. J Biol Chem. 1992;267:13073–8.
11. Bhandari V, Palfree RG, Bateman A. Isolation and sequence of the granulin precursor cDNA from human bone marrow reveals tandem cysteine-rich granulin domains. Proc. Natl. Acad. Sci. U.S.A. 1992; 89:1715–9.
12. Salazar DA, Butler VJ, Argouarch AR, Hsu TY, Mason A, Nakamura A, et al. The Progranulin Cleavage Products, Granulins, Exacerbate TDP-43 Toxicity and Increase TDP-43 Levels. J Neurosci. 2015;35:9315–28.
13. Thurner L, Fadle N, Regitz E, et al. The molecular basis for development of proinflammatory autoantibodies to progranulin. J Autoimmun. 2015;61:17–28.
14. Butler VJ, Cortopassi WA, Gururaj S, et al. Multi-Granulin Domain Peptides Bind to Pro-Cathepsin D and Stimulate Its Enzymatic Activity More Effectively Than Progranulin in Vitro. Biochemistry. 2019;58(23):2670–4.
15. Suh H-S, Choi N, Tarassishin L, Lee SC. Regulation of Progranulin Expression in Human Microglia and Proteolysis of Progranulin by Matrix Metalloproteinase-12 (MMP-12). Combs C, editor. PLoS ONE. 2012;7: e35115.
16. Hu F, Padukkavidana T, Vægter CB, Brady OA, Zheng Y, Mackenzie IR, et al. Sortilin-Mediated Endocytosis Determines Levels of the Frontotemporal Dementia Protein, Progranulin. Neuron. Elsevier Inc; 2010; 68:654–67.
17. Lee CW, Stankowski JN, Chew J, Cook CN, Lam Y-W, Almeida S, et al. The lysosomal protein cathepsin L is a progranulin protease. Molecular Neurodegeneration. 2017;12:55.
18. Tanaka Y, Matsuwaki T, Yamanouchi K, Nishihara M. Increased lysosomal biogenesis in activated microglia and exacerbated neuronal damage after traumatic brain injury in progranulin-deficient mice. Neuroscience. 2013;250:8–19.
19. Holler CJ, Taylor G, Deng Q, Kukar T. Intracellular Proteolysis of Progranulin Generates Stable, Lysosomal Granulins That Are Haploinsufficient in Patients with Frontotemporal Dementia Caused by GRN Mutations. eNeuro. 2017; ENEURO.0100–17.2017.

20. Zhou X, Paushter DH, Feng T, Sun L, Reinheckel T, Hu F. Lysosomal processing of progranulin. Molecular Neurodegeneration. 2017;12:62.
21. Nguyen AD, Nguyen TA, Cenik B, et al. Secreted progranulin is a homodimer and is not a component of high-density lipoproteins (HDL). J Biol Chem. 2013;288(12):8627–35.
22. Sanjana NE, Shalem O, Zhang F. Improved vectors and genome-wide libraries for CRISPR screening. Nat Methods. 2014;11(8):783–4.
23. Bordeaux J, Welsh A, Agarwal S, et al. Antibody validation [published correction appears in Biotechniques. 2010 May;48(5):351]. Biotechniques. 2010;48(3):197–209.
24. Rosenfeld J, Capdevielle J, Guillemot JC, Ferrara P. In-gel digestion of proteins for internal sequence analysis after one- or two-dimensional gel electrophoresis. Anal Biochem. 1992;203:173–9.
25. Hellman U, Wernstedt C, Góñez J, Heldin CH. Improvement of an “In-Gel” digestion procedure for the micropreparation of internal protein fragments for amino acid sequencing. Anal Biochem. 1995;224:451–5.
26. Baker PR, Chalkley RJ. MS-viewer: a web-based spectral viewer for proteomics results. Mol Cell Proteomics. 2014;13:1392–6.
27. Turk V, Stoka V, Vasiljeva O, Renko M, Sun T, Turk B, et al. Biochimica et Biophysica Acta. BBA - Proteins and Proteomics. Elsevier BV. 2012;1824:68–88.
28. Banay-Schwartz M, Bracco F, Dahl D, Deguzman T, Turk V, Lajtha A. The pH dependence of breakdown of various purified brain proteins by cathepsin D preparations. Neurochem. Int. 1985;7:607–14.
29. Turk B, Dolenc I, Lenarcic B, Krizaj I, Turk V, Bieth JG, et al. Acidic pH as a physiological regulator of human cathepsin L activity. Eur J Biochem. 1999;259:926–32.
30. Rossi A, Deveraux Q, Turk B, Sali A. Comprehensive search for cysteine cathepsins in the human genome. Biol Chem. 2004;385:363–72.
31. Dall E, Brandstetter H. Structure and function of legumain in health and disease. Biochimie Elsevier BV. 2016;122:126–50.
32. Jordans S, Jenko-Kokalj S, Kühl NM, Tedelind S, Sendt W, Brömme D, et al. Monitoring compartment-specific substrate cleavage by cathepsins B, K, L, and S at physiological pH and redox conditions. BMC Biochem. 2009;10:23.
33. Zaidi N, Kalbacher H. Cathepsin E. A mini review. Biochem Biophys Res Commun. 2008;367:517–22.
34. Stoka V, Turk V, Turk B. Lysosomal cathepsins and their regulation in aging and neurodegeneration. Ageing Res Rev. 2016;32:22–37.
35. Valdez C, Wong YC, Schwake M, Bu G, Wszolek ZK, Krainc D. Progranulin-mediated deficiency of cathepsin D results in FTD and NCL-like phenotypes in neurons derived from FTD patients. Hum Mol Genet. 2017;26:4861–72.
36. Zhou X, Paushter DH, Feng T, Pardon CM, Mendoza CS, Hu F. Regulation of cathepsin D activity by the FTLD protein progranulin. 134. Berlin Heidelberg: Acta Neuropathologica. Springer; 2017.

pp. 151–3.
37. Beel S, Moisse M, Damme M, De Muynck L, Robberecht W, Van Den Bosch L, et al. Progranulin functions as a cathepsin D chaperone to stimulate axonal outgrowth in vivo. Hum Mol Genet. 2017;26:2850–63.
38. Ward ME, Chen R, Huang H-Y, Ludwig C, Telpoukhovskaia M, Taubes A, et al. Individuals with progranulin haploinsufficiency exhibit features of neuronal ceroid lipofuscinosis. Sci Transl Med. 2017;9.
39. Butler VJ, Cortopassi WA, Argouarch AR, Ivry SL, Craik CS, Jacobson MP, et al. Progranulin Stimulates the In Vitro Maturation of Pro-Cathepsin D at Acidic pH. Journal of Molecular Biology. Elsevier Ltd; 2019;1–10.
40. Sun H, Lou X, Shan Q, Zhang J, Zhu X, Zhang J, et al Proteolytic Characteristics of Cathepsin D Related to the Recognition and Cleavage of Its Target Proteins. Hess S, editor. PLoS ONE. 2013;8: e65733.
41. Yamashita Y, Nagasaka T, Naiki-Ito A, Sato S, Suzuki S, Toyokuni S, et al. Napsin A is a specific marker for ovarian clear cell adenocarcinoma. Nature Publishing Group. 2014;28:111–7.
42. Uchida A, Samukawa T, Kumamoto T, Ohshige M, Hatanaka K, Nakamura Y, et al. Napsin A levels in epithelial lining fluid as a diagnostic biomarker of primary lung adenocarcinoma. BMC Pulmonary Medicine; 2017;1–9.
43. Korkmaz B, Horwitz MS, Jenne DE, Gauthier F. Neutrophil, Elastase. Proteinase 3, and Cathepsin G as Therapeutic Targets in Human Diseases. Pharmacol Rev. 2010;62:726–59.
44. Zhang Y, Sloan SA, Clarke LE, Caneda C, Plaza CA, Blumenthal PD, et al. Purification and Characterization of Progenitor and Mature Human Astrocytes Reveals Transcriptional and Functional Differences with Mouse. Neuron. Elsevier Inc; 2016; 89:37–53.45.
45. Butler VJ, Gao F, Corrales CI, et al. Age- and stress-associated C. elegans granulins impair lysosomal function and induce a compensatory HLH-30/TFEB transcriptional response. PLoS Genet. 2019;15(8):e1008295.
46. Chen-Plotkin AS, Xiao J, Geser F, Martinez-Lage M, Grossman M, Unger T, et al. Brain progranulin expression in GRN-associated frontotemporal lobar degeneration. Acta Neuropathol. 2009;119:111–22.
47. Olson OC, Joyce JA. Cysteine cathepsin proteases: regulators of cancer progression and therapeutic response. Nat Rev Cancer. 2015;15(12):712–29.
48. Alquezar C, Esteras N, la Encarnación de A, Moreno F, López de Munain A, Martín-Requero Á. Increasing progranulin levels and blockade of the ERK1/2 pathway: upstream and downstream strategies for the treatment of progranulin deficient frontotemporal dementia. Eur Neuropsychopharmacol. 2015;25:386–403.
49. la Encarnación de A, Alquezar C, Esteras N, Martín-Requero Á. Progranulin Deficiency Reduces CDK4/6/pRb Activation and Survival of Human Neuroblastoma SH-SY5Y Cells. Mol Neurobiol. 2014;52:1714–25.

50. Chen JM, Dando PM, Rawlings ND, Brown MA, Young NE, Stevens RA, et al. Cloning, isolation, and characterization of mammalian legumain, an asparaginyl endopeptidase. J Biol Chem. 1997;272:8090–8.
51. Rosenmann H. Asparagine endopeptidase cleaves tau and promotes neurodegeneration. Nature Medicine Nature Publishing Group. 2014;20:1236–8.
52. Zhang Z, Song M, Liu X, Kang SS, Kwon I-S, Duong DM, et al. Cleavage of tau by asparagine endopeptidase mediates the neurofibrillary pathology in Alzheimer's disease. Nature Medicine. 2014;20:1254–62.
53. Herskowitz JH, Gozal YM, Duong DM, Dammer EB, Gearing M, Ye K, et al. Asparaginyl endopeptidase cleaves TDP-43 in brain. Lubec G, editor. Proteomics. 2012; 12:2455–63.
54. Hawdon JM, Emmons SW, Jacobson LA. Regulation of proteinase levels in the nematode Caenorhabditis elegans. Preferential depression by acute or chronic starvation. Biochem J. 1989;264(1):161–5.

Tables

Due to technical limitations, tables 1-2 are only available as downloads in the supplemental files section.

Table 1. PGRN cleavage by lysosomal proteases *in vitro*

Summary of whether the enzymes tested could cleave progranulin (PGRN) or not along with the potential compartment it may cleave PGRN depending on the pH it processed progranulin *in vitro*. En, endosomes; Ly, lysosomes; Ex, extracellular.

Table 2. Clinical Information for control and FTLD-TDP-*Pgrn* subjects

Clinical information for the control and FTLD-TDP-*Pgrn* subjects. PMI, post-mortem interval; IOC, inferior occipital cortex; MFG, middle frontal gyrus.

Figures

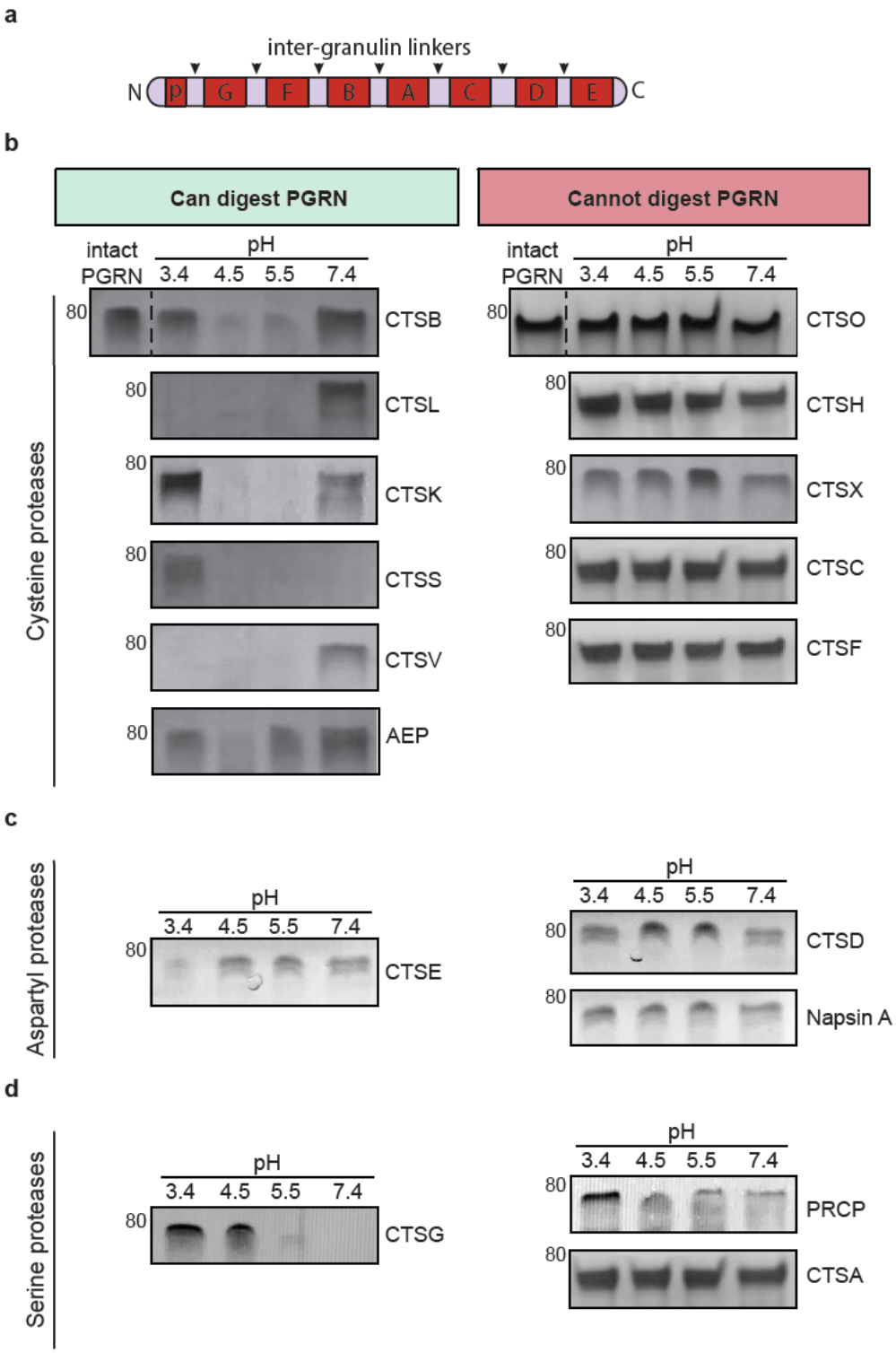

Figure 1

Progranulin can be digested by multiple lysosomal proteases in vitro a, Schematic representation of progranulin (PGRN) protein. Black arrows indicate inter-granulin linkers, individual granulins named granulins A-G (~7kD each) and paragranulin (p) (~3.5kD) are annotated. b, c, d, 1μM of each enzyme was incubated with 400ng of recombinant human PGRN at the indicated pH for 20 minutes. The proteins were

silver stained (shown in greyscale) to assess the presence or absence of PGRN at every condition. Also see Table 1 and Fig. 3. All assays were repeated n=3 times.

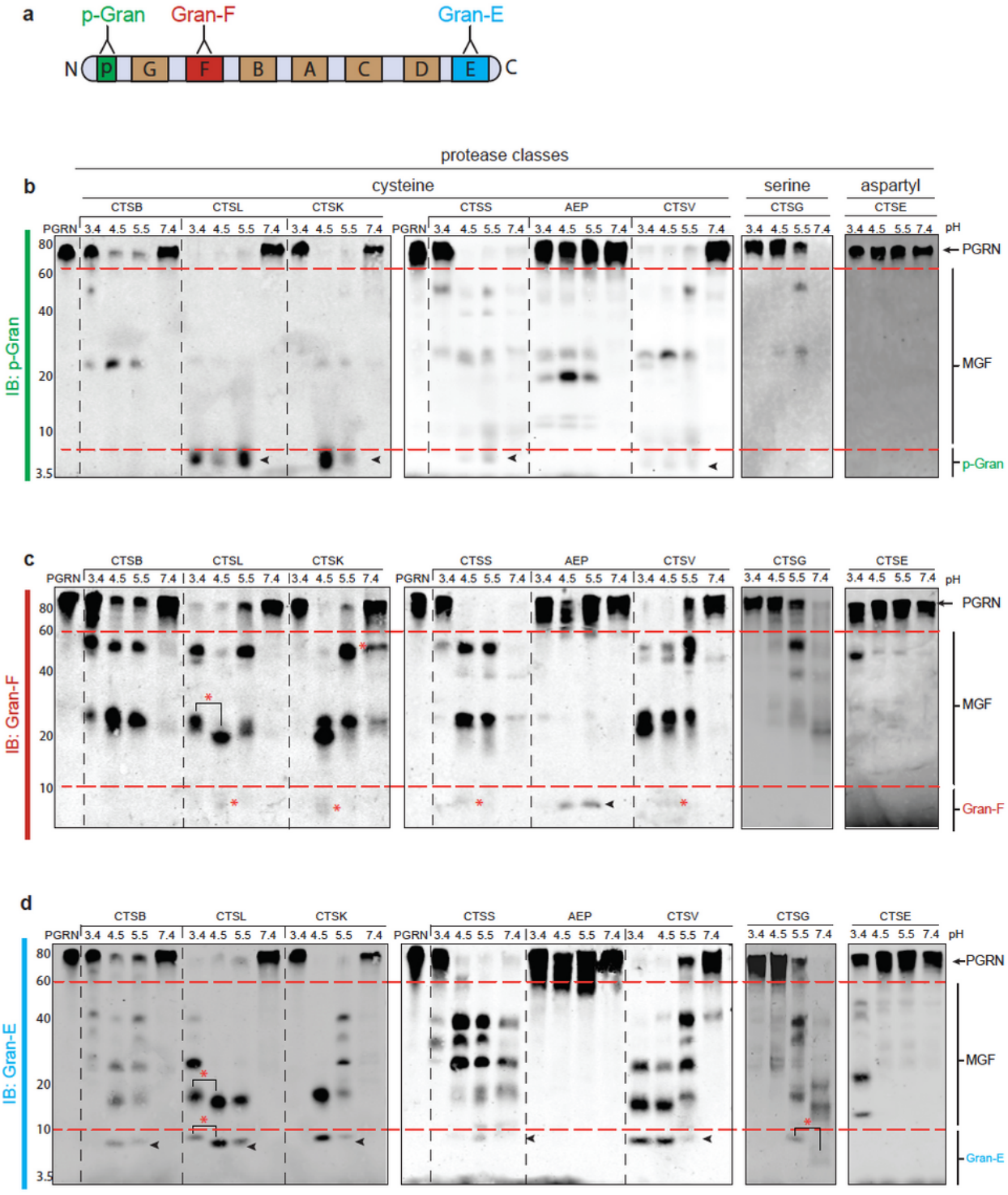

Figure 2

PGRN undergoes pH-dependent processing into multi-granulin fragments and individual granulins in vitro a, Schematic representation of the antibodies used. N-terminus, paragranulin (p-Gran) in green, middle, granulin F (Gran-F) in red and C-terminus, granulin E (Gran-E) in blue. b-d, 400ng of PGRN was incubated

with or without 1μM of each enzyme at indicated pH for 20 minutes. Western blotting analysis was performed using each antibody (b, P-Gran, c, Gran-F and d, Gran-E) to assess the results of the in vitro assay. pH-dependent changes are indicated with *. PGRN, progranulin; MGF, multi-granulin fragments; CTSB, cathepsin B; CTSL, cathepsin L; CTSK, cathepsin K; CTSS, cathepsin S; AEP, asparagine endopeptidase; CTSV, cathepsin V; CTSG, cathepsin G; CTSE, cathepsin E. All assays were repeated n=3 times. Also see Fig. S3, S4 and S5)

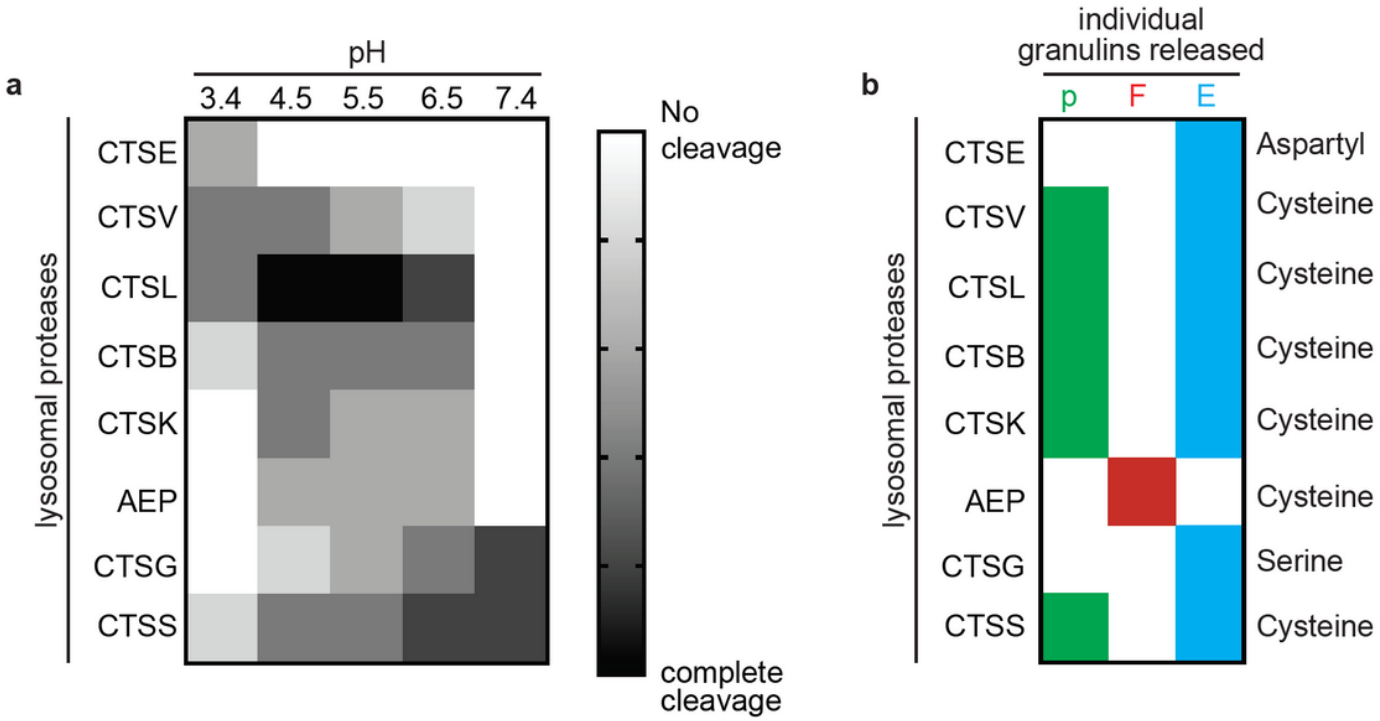

Figure 3

PGRN processing into granulins by multiple proteases is pH dependent Summary of the results of the in vitro assays. a, Processing of PGRN to granulins by different proteases is dependent on pH. The range of cleavage is represented in greyscale with no cleavage in white and complete cleavage in black. The range takes into account the amount of full-length PGRN processed into multi-granulin fragments and individual granulins within 20 minutes. b, Represented is the ability of each enzyme to liberate individual paragranulin (p) in red, granulin F (F) in green, and granulin E (E) in blue. The protease classes are also indicated. CTSE, cathepsin E; CTSV, cathepsin V; CTSL, cathepsin L; CTSB, cathepsin B; CTSK, cathepsin K; AEP, asparagine endopeptidase; CTSG, cathepsin G; CTSS, cathepsin S.

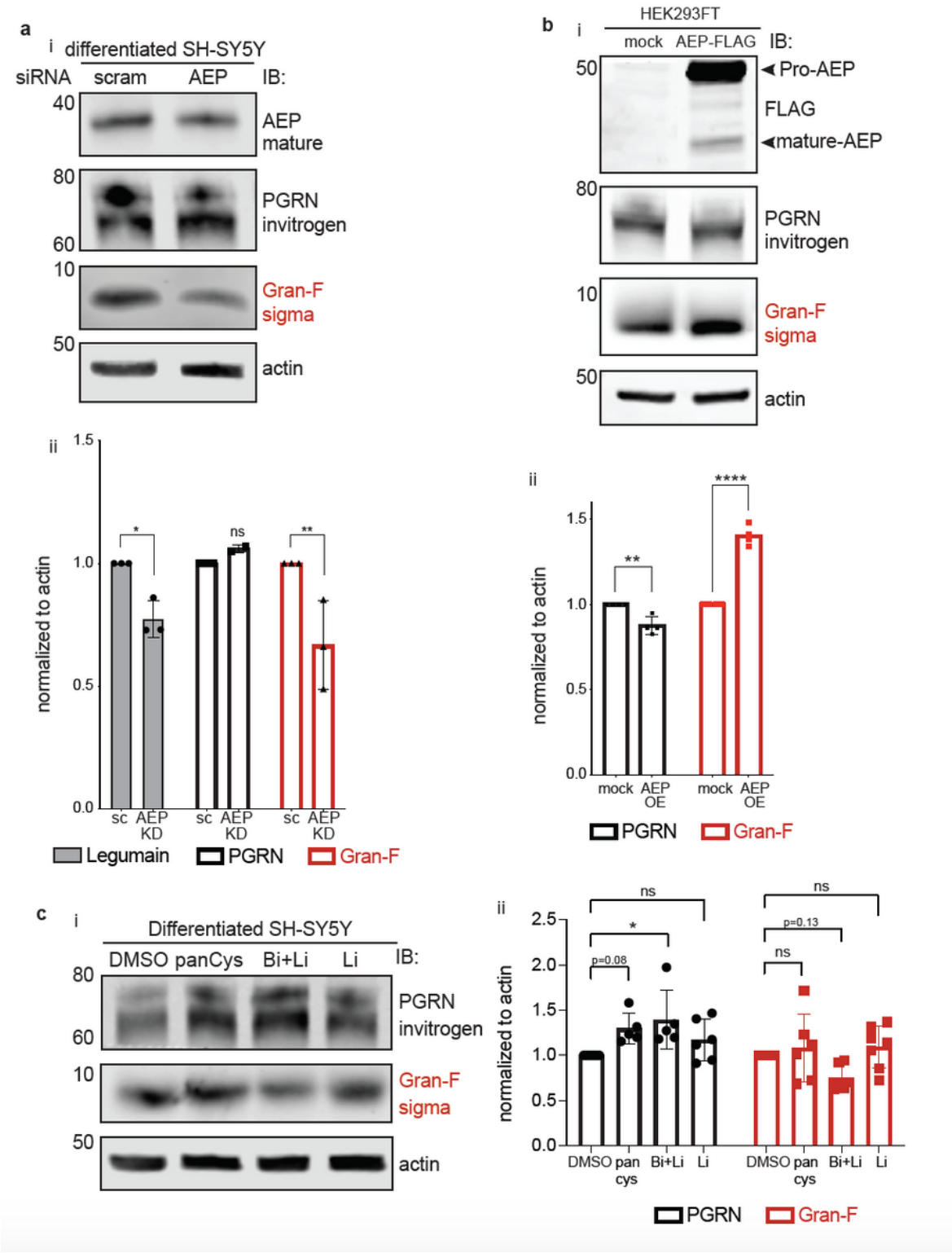

Figure 4

Asparagine endopeptidase is a PGRN protease that liberates granulin F a, Differentiated SH-SY5Y cells were treated with siRNA against AEP or scramble control for 60 hours. Cells were lysed and blotted for endogenous AEP, PGRN and Gran-F using the antibodies indicated. Quantification was performed compared to scramble-treated control. Mature AEP levels (**p=0.006). endogenous PGRN levels, ns, not significant. Quantification of Gran-F levels (*p=0.03). Error bars represent mean with standard deviation.

Unpaired student's t-test performed for statistical significance with assuming both groups have the same standard deviation. Experiment was repeated n=3. b, HEK293FT cells were transiently transfected with FLAG-tagged AEP or empty FLAG vector for 24 hours and cells lysates were probed for endogenous PGRN and Gran-F using the antibodies stated. over-expression was confirmed using a FLAG antibody. Quantification was performed compared to mock controls. Quantification of endogenous PGRN (**p=0029) and Gran-F (****p<0.0001). Experiments were repeated N=4. Error bars represent mean with standard deviation. Unpaired student's t-test performed for statistical significance with assuming both groups have the same standard deviation. c, Differentiated SH-SY5Y cells were treated with DMSO, 10μM E64D (pan-cysteine protease inhibitor - panCys), 15μM CA074_ME (CTSB and CTSL dual-inhibitor – Bi+Li) and 10μM of CTSLi II (CTSL inhibitor – Li) for 24 hours. 24 hours post-inhibition cells were lysed and probed for endogenous PGRN and granulin F. Quantification of endogenous PGRN (*p=0.0178) and Gran-F compared to vehicle-treated controls. Experiments were repeated N=6. Error bars represent mean with standard deviation. One-way ANOVA test was performed for significance and Dunnett's test was used to correct for multiple comparison. ns, not significant

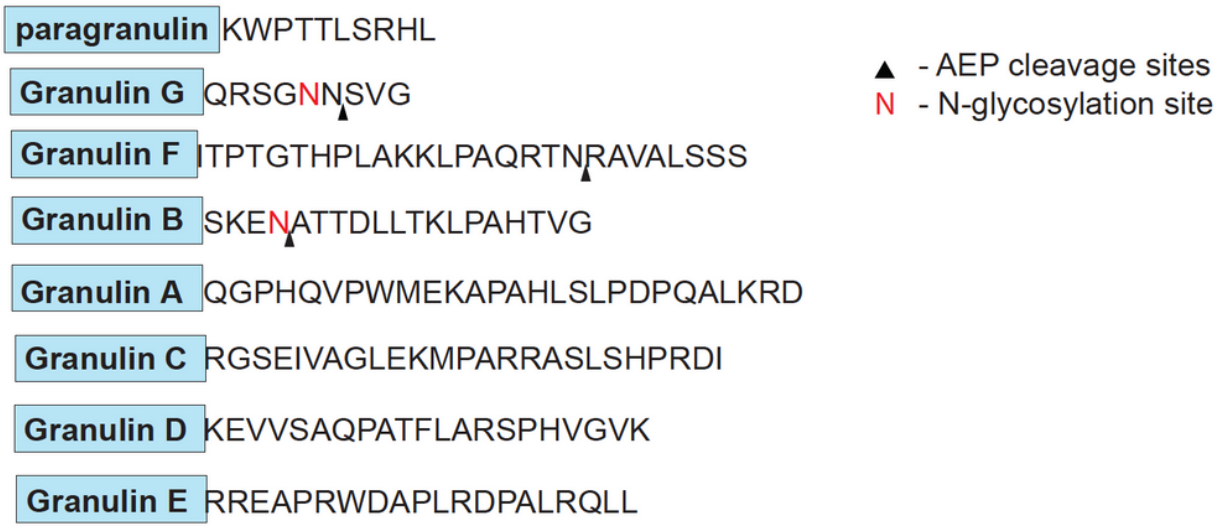

Figure 5

Asparagine endopeptidase liberates granulin F from PGRN Visual representation of PGRN protein with the individual granulin domains annotated in blue boxes with their associated C-terminal inter-granulin linker following. AEP cleavage sites are indicated with . N, represents N-linked glycosylation sites. (also see Fig. S9). PGRN, progranulin; Gran-F, granulin F

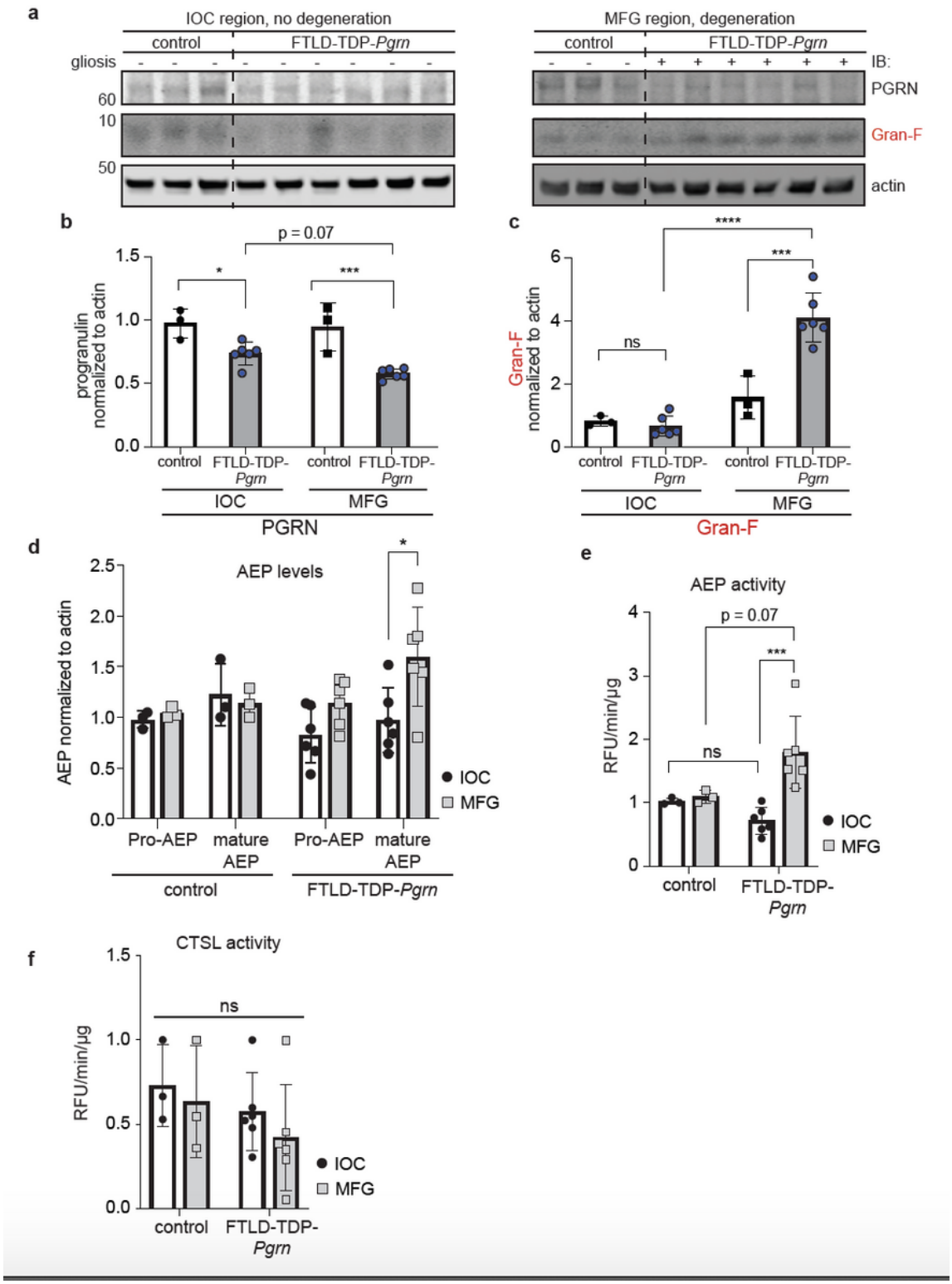

Figure 6

Granulins F levels are increased in the degenerating regions of the brain from FTLD-TDP-Pgrn patients a, Western blot analysis for endogenous PGRN and Gran-F from the brain lysates. b, Quantification of PGRN levels in both IOC and MFG regions in FTLD-TDP-Pgrn patients compared to the same regions in control subjects (*, p=0.023, ***, p<0.0005). c, Quantification of Gran-F levels in both IOC and MFG regions in FTLD-TDP-Pgrn patients and controls (***p=0.0001, ****p<0.0001). Error bars represent mean with

standard deviation. One-way ANOVA was performed for statistical significance and Tukey's test was performed to correct for multiple comparisons. d, Western blot analysis of endogenous AEP levels. Quantification of pro and mature AEP levels in both IOC and MFG regions in FTLD-TDP-Pgrn patients compared to the same regions in control subjects (*, p=0.026). Two-way ANOVA performed for statistical significance and Tukey's test was performed to correct for multiple comparisons. e, AEP activity in both IOC and MFG regions in FTLD-TDP-Pgrn patients compared to the same regions in controls (***p=0.0008) One-way ANOVA was performed for statistical significance and Tukey's test was performed to correct for multiple f, CTSL activity in both IOC and MFG regions in FTLD-TDP-Pgrn patients compared to the same regions in controls. ns, not significant. One-way ANOVA was performed for statistical significance and Tukey's test was performed to correct for multiple comparisons. Control n = 3, FTLD-TDP-Pgrn n = 6. Also see Table 2. PGRN, progranulin; Gran-F, granulin F.

Supplementary Files

This is a list of supplementary files associated with this preprint. Click to download.

- SUPPLEMENTALFIGURESMohanetal.FINAL.pdf
- AppendixFigureMohanetal.FINAL.pdf
- TABLESMohanetal.FINAL.pdf